Rare Decays of K_L and π^0 to Leptons.

Amitabh Lath
for the KTeV Collaboration
Rutgers University

We present preliminary branching ratio measurements of the rare decays $\pi^0 \to 2e$, $\pi^0 \to 4e$, $K_L \to 4e$ as well as a significant observation of $K_L \to e^+e^-\mu^+\mu^-$ from data taken during the 1997 run of KTeV/E799II. These decays probe the $\gamma^*\gamma^*$ form factor of the π^0 and K_L. The $K_L\gamma^*\gamma^*$ form factor is useful in understanding the long-distance contribution to the decay $K_L \to \mu^+\mu^-$. Our measurement of the $\pi^0 \to 2e$ branching ratio constitutes the first significant measurement of the excess over the QED unitarity limit. All these analyses represent at least an order of magnitude increase in statistics over previously published results. In the case of $K_L \to e^+e^-\mu^+\mu^-$, our observations solidify the previous observation (made by E799I), which was based on one event.

I. INTRODUCTION

Rare decays of K_L and π^0 mesons are improtant for the study of phenomena at high energy scales. Especially important are the $\gamma^*\gamma^*$ vertices which dominate the decays of the mesons into two and four leptons. The $K_L \to \mu^+\mu^-$ branching ratio [1] is understood to have a *short distance* component (decays involving W,Z bosons) which are sensitive the CKM matrix element V_{td}, and a *long distance* component, consisting of $K_L\gamma\gamma$ vertex, in which the γ can be on shell (unitarity limit) or off shell.

The four-lepton decay modes of the K_L proceed through the $K_L\gamma^*\gamma^*$ vertex and can, in principle, be used to extract the short distance information from $K_L \to \mu^+\mu^-$. They are also of significant interest in their own right, as the angle between the lepton-pair planes is sensitive to CP-violation. The two and four lepton decay modes of the π^0 are also interesting since they probe the $\pi^0\gamma^*\gamma^*$ vertex.

II. THE KTEV DETECTOR.

The KTeV experiment, as configured for rare decay searches (E799II) used two nearly parallel kaon beams created by 800 GeV protons incident on a BeO target. The kaon decays used in our studies were collected in a decay region approximately 60 meters long, situated approximately 100 meters from the production target. The charged particles were detected by four drift chambers arranged on either side of an analysis magnet, followed by a trigger hodoscope bank and a 3100 element pure CSI calorimeter. Two banks of hodoscopes which served to tag muon tracks were situated downstream of the calorimeter, separated by a Pb wall and several meters of steel.

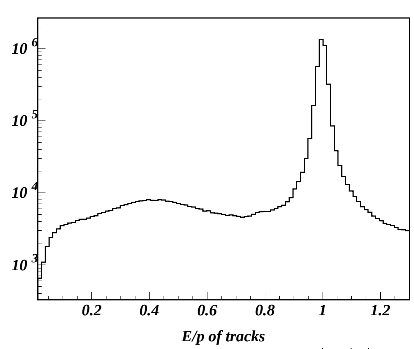

FIG. 1. The calorimeter energy vs the track momentum (E/p). Electron are in the peak at 1.0.

The calorimeter was used to identify tracks as $e^{\pm}$. The ratio of the energy deposited in the calorimeter vs. the momentum measured by the tracking system (E/p) is shown in figure 1 for events cosisting primarily of $K_L \to \pi^{\pm} e^{\mp} \nu$. The $e^{\pm}$ tracks, in the peak at $E/p \sim 1.0$, can be isolated with negligible background from tracks due to $\pi^{\pm}$, which are in a broad distribution at lower E/p.

III. PROBING $K_L\gamma^*\gamma^*$ VIA DECAYS TO FOUR LEPTONS.

The $K_L\gamma^*\gamma^*$ vertex can be probed by studying decays of the K_L to four leptons. Figure 2 shows the $K_L\gamma^*\gamma^*$ vertex as it contributes to the process $K_L \to \mu^+\mu^-$, as well as the process $K_L \to l_1^+ l_1^- l_2^+ l_2^-$ ($l_1 = e, l_2 = e, \mu$). If the contribution of this vertex can be determined, then the short distance part of the decay may be isolated. The absorbtive contribution can be determined from the decay $K_L \to \gamma\gamma$.

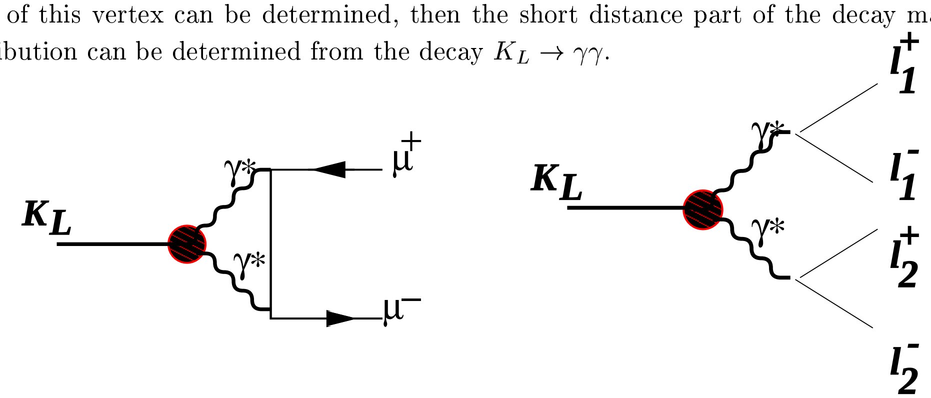

FIG. 2. The contribution of the vertex $K_L\gamma^*\gamma^*$ to the process $K_L \to \mu^+\mu^-$ (left), as well as to $K_L \to l_1^+ l_1^- l_2^+ l_2^-$ ($l_1 = e, l_2 = e, \mu$) (right).

A. The Decay $K_L \to e^+e^-\mu^+\mu^-$.

The decay $K_L \to e^+e^-\mu^+\mu^-$ offers the best window onto the $K_L\gamma^*\gamma^*$ vertex. However, the decay is rare, E799I measured BR($K_L \to e^+e^-\mu^+\mu^-$) $= 2.9 \times 10^{-9}$ [2] with one event.

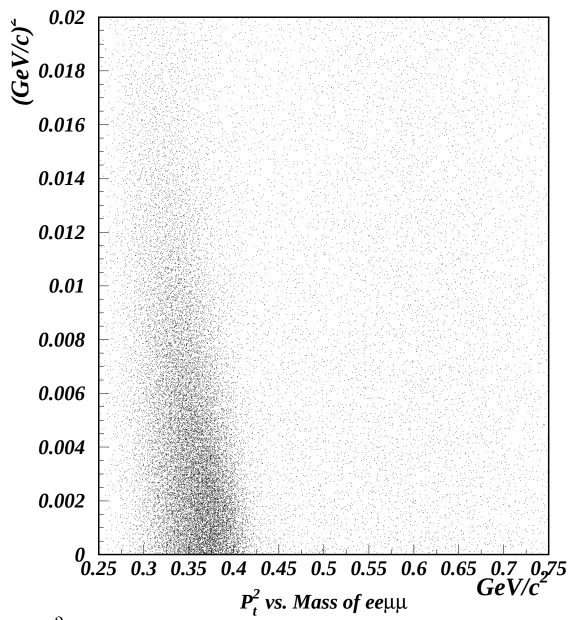

FIG. 3. The P_t^2 vs. $M_{ee\mu\mu}$ for data events with two muons and two electrons.

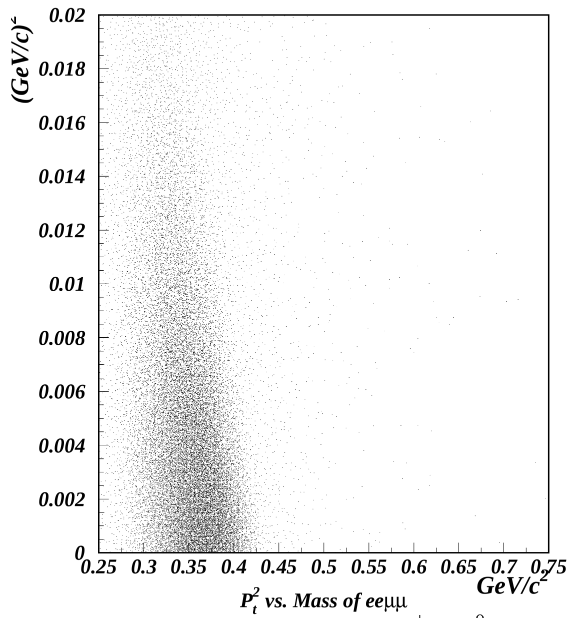

FIG. 4. The P_t^2 vs. $M_{ee\mu\mu}$ for Monte Carlo simulation of $K_L \to \pi^+\pi^-\pi^0_D$ with charged pion punchthrough/decay.

Figure 3 shows the distribution of transverse momentum (P_t^2) vs. $M_{ee\mu\mu}$ for events with four tracks, two identified as muons (with tracks extrapolated to hits in the muon counters), and two identified as electrons (using E/P in the CSI calorimeter). The contribution from the decay $K_L \to \pi^+\pi^-\pi^0$ in which the π^0 undergoes a dalitz decay (π^0_D), and the charged pion punchthrough the steel, or decay, is noticable as a band centered at $M_{ee\mu\mu} \sim 0.35\mathrm{GeV/c}^2$, and constitutes the main background to this decay. Figure 4 shows a similar plot for Monte Carlo simulation of the decay $K_L \to \pi^+\pi^-\pi^0_D$ with charged pion punchthrough/decay. This agreement of the background simulation and the data is also shown in figure 5, in a one-dimensional plot of $M_{ee\mu\mu}$. The data at high mass are due to events in which two K_L decays were recorded in the same event. These double decay events can be eliminated by requiring all four tracks to originate from the same vertex.

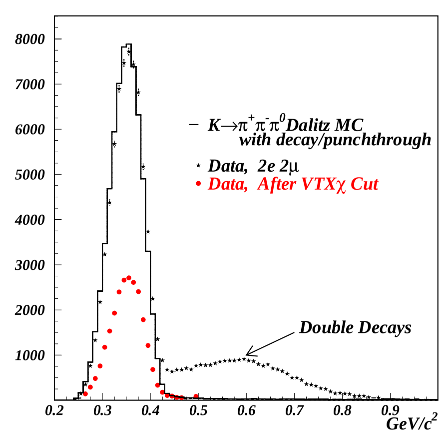

FIG. 5. The distribution of $M_{ee\mu\mu}$ for Monte Carlo simulation of $K_L \to \pi^+\pi^-\pi^0_D$ with charged pion punchthrough/decay (line), as well as data without cuts (stars) and data in which a good 4-track vertex has been found (dots).

The background from $K_L \to \pi^+\pi^-\pi^0_D$ was reduced by removing events which contained an extra photon-like cluster in the calorimeter, presumably from the $\pi^0 \to e^+e^-\gamma$ decay. Cuts on a combination of M_{ee} and track separation at the first drift chamber serve to remove $K_L \to \mu^+\mu^-\gamma$ events in which the γ converts to e^+e^- pair at the vacuum window. The final P_t^2 vs $M_{ee\mu\mu}$ shown in figure 6 shows 38 signal events within the signal box given by $0.48 \leq M_{ee\mu\mu} \leq 0.51$ GeV/c^2 and $P_t^2 \leq 250$ (MeV/c)^2. Figure 7 shows the $M_{ee\mu\mu}$ distribution for $P_t^2 \leq 250$ (MeV/c)^2.

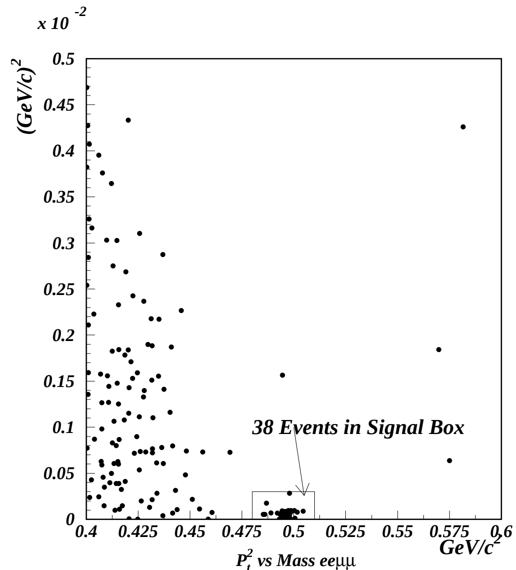

FIG. 6. P_t^2 vs. $M_{ee\mu\mu}$ for $K_L \to e^+e^-\mu^+\mu^-$, with all cuts. There are 38 events in the signal box.

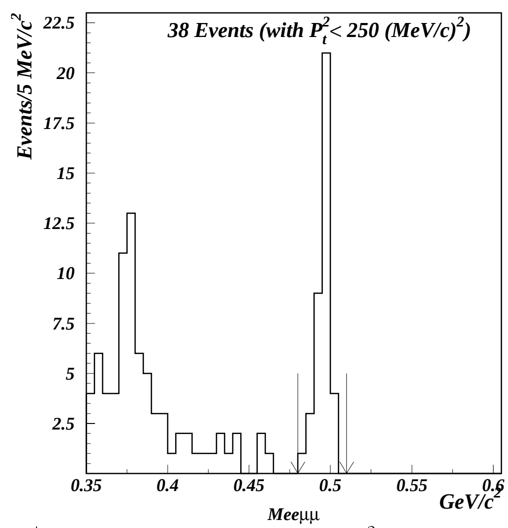

FIG. 7. $M_{ee\mu\mu}$ for $K_L \to e^+e^-\mu^+\mu^-$, with all cuts, including $P_t^2 \leq 250$ (MeV/c)^2. The peak at M_K is evident.

B. The Decay $K_L \to e^+e^-e^+e^-$.

The decay $K_L \to e^+e^-e^+e^-$ has a higher branching ratio than $K_L \to e^+e^-\mu^+\mu^-$, but suffers from the confusion of having similar particles from decays mediated by the γ^*.

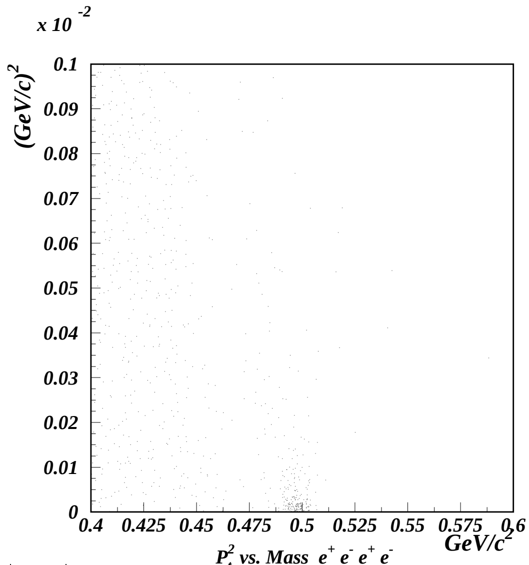

FIG. 8. P_t^2 vs. $M_{ee\mu\mu}$ for $K_L \to e^+e^-e^+e^-$, with all cuts. There is very little background. The signal is evident at M_K and $P_t^2 \sim 0$.

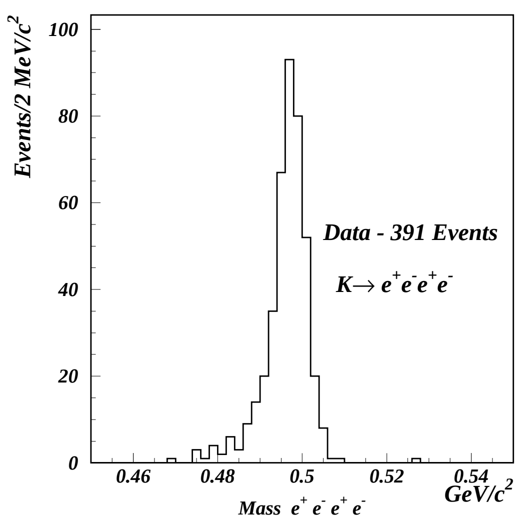

vskip -.2 cm

FIG. 9. M_{eeee} for $K_L \to e^+e^-e^+e^-$, with all cuts, including $P_t^2 \leq 250$ (MeV/c)^2. The peak at M_K is contains 391 events.

Figure 8 shows the P_t^2 vs. M_{eeee} for the decay $K_L \to e^+e^-e^+e^-$, with all cuts. The signal events at $M_{eeee} \sim 0.498\text{GeV/c}^2$ are evident at $P_t^2 \sim 0$. Figure 9 shows the M_{eeee} distribution for $P_t^2 \leq 250$ (MeV/c)^2. The 391 signal events are well separated from backgrounds. The best previous observation of this decay [2] was made with 27 events.

The preliminary BR($K_L \to e^+e^-e^+e^-$) is $(4.14 \pm 0.27 \text{ (stat)} \pm 0.31 \text{ (sys)}) \times 10^{-8}$. There are various predictions: 3.68×10^{-8} [3], 3.73×10^{-8} [4], and 3.8×10^{-8} [5]. All of these predictions are consistent with the KTeV preliminary result.

IV. THE DECAYS $\pi^0 \to E^+E^-$ AND $\pi^0 \to E^+E^-E^+E^-$.

The decay $K_L \to 3\pi^0$ provides KTeV with a copious source of π^0. Figure 10 shows fully reconstructed $K_L \to 3\pi^0$ decays containing four electrons, either from the decay $\pi^0 \to e^+e^-e^+e^-$, or from two $\pi^0 \to e^+e^-\gamma$ decays.

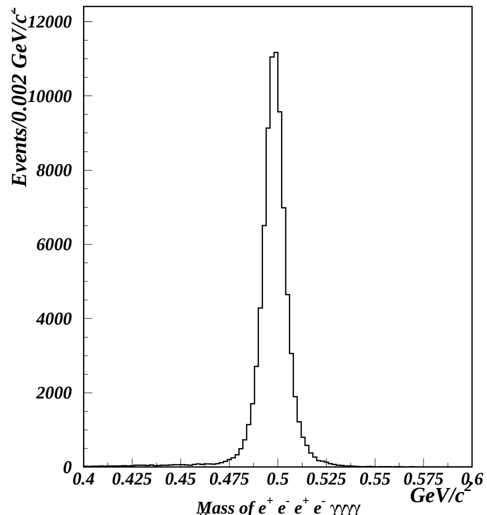

FIG. 10. $M_{eeee\gamma\gamma\gamma}$ from fully reconstructed $K_L \to 3\pi^0$, for events containing four electrons, from the decay $\pi^0 \to e^+e^-e^+e^-$ as well as two $\pi^0 \to e^+e^-\gamma$.

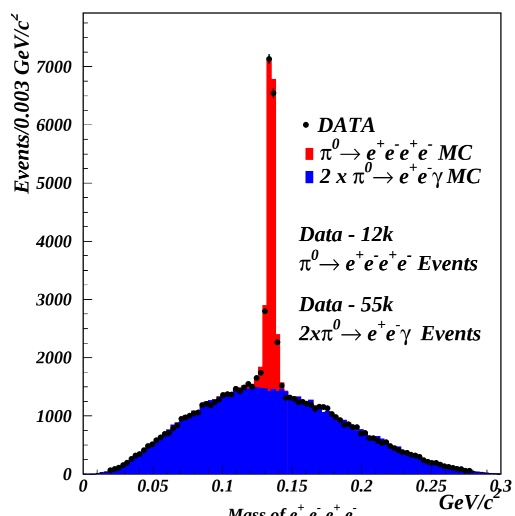

FIG. 11. M_{eeee} from fully reconstructed $K_L \to 3\pi^0$ The peak due to $\pi^0 \to e^+e^-e^+e^-$ is evident at M_{π^0}. The dots show data, the shaded distributions show the 4e and $2\pi^0$ Dalitz background. The 4e decays can be isolated with ~2.8% background.

Figure 11 shows the distribution for M_{eeee}. The peak at M_{π^0} is due to the decay $\pi^0 \to e^+e^-e^+e^-$. There is a broad background due to two decays π^0 to $e^+e^-\gamma$. A χ^2-like quantity using the reconstructed π^0 masses using the various electron and photon combinations was used to separate the $\pi^0 \to e^+e^-e^+e^-$ from the background. Approximately 12,000 events, with a background of $\sim 2.8\%$ were isolated. This is to be compared to the best previous sample of 146 events seen by [6]. The preliminary branching ratio is measured to be $\frac{\Gamma(\pi^0 \to e^+e^-e^+e^-)}{\Gamma(\pi^0 \to \gamma\gamma)} = (3.31 \pm 0.04(stat) \pm 0.22(sys)) \times 10^{-5}$

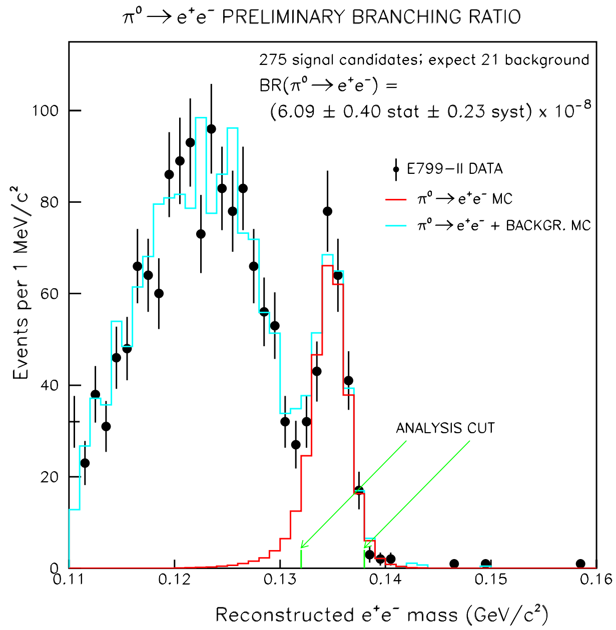

FIG. 12. M_{ee} from fully reconstructed $K_L \to 3\pi^0$. The dots show the data, while the solid lines show the Monte Carlo simulation of the signal and the dominant background. The arrows indicate the signal region.

Figure 12 shows the distribution for $M_{e^+e^-}$. The peak due to $\pi^0 \to e^+e^-$ is clearly evident at M_{π^0}. There are 275 signal candidates with a background expectation (chiefly from $\pi^0 \to e^+e^-\gamma$ decays) of 21 events. The branching ratio is measured to be $BR(\pi^0 \to e^+e^-) = (6.09 \pm 0.40 \text{ (stat)} \pm 0.23 \text{ (sys)}) \times 10^{-8}$, with $m_{e^+e^-}/m_{\pi^0} > 0.95$. This is in reasonably good agreement with the prediction of Amteller et al [7] of 6.41×10^{-8}, and in disagreement with the prediction by Gomez Dumm et al [8] of 8.3×10^{-8}. This measurement establishes the branching ratio of $\pi^0 \to e^+e^-$ $> 4\sigma$ above the unitarity limit.

V. CONCLUSION

We have shown the first clear peak of the rare decay $K_L \to e^+e^-\mu^+ mu^-$ with 38 events. We have a sample of $\sim$ 400 events for the decay $K_L \to e^+e^-e^+e^-$ and have measured a preliminary branching ratio of $(4.14 \pm 0.27 \text{ (stat)} \pm 0.31 \text{ (sys)}) \times 10^{-8}$. Further understanding of these $K_L\gamma^*\gamma^*$ mediated decays could lead to an improved determination of the CKM matrix element V_{td}.

In addition, we have $\sim$ 12,000 $\pi^0 \to 4e$ sample events, and have measured a preliminary branching ratio $\frac{\Gamma(\pi^0 \to e^+e^-e^+e^-)}{\Gamma(\pi^0 \to \gamma\gamma)} = (3.31 \pm 0.04(stat) \pm 0.22(sys)) \times 10^{-5}$ For the rare decay $\pi^0 \to e^+e^-$ we have made a measurement of the branching ratio, the first to show it to be significantly above the unitarity limit. The KTeV result is $(6.09 \pm 0.40 \text{ (stat)} \pm 0.23 \text{ (sys)}) \times 10^{-8}$.

[1] R. Lee for BNL E871, these proceedings.
[2] P. Gu et. al., Phys. Rev. Lett. **72**, 3000 (1994)
[3] Miyazaki, Takasugi, Phys Rev. **D8** 2051 (1973)
[4] Quigg, Jackson, UCRL-18487 (1968)
[5] L. Zhang, J.L. Goity, PRD **57**, 7031 (1998)
[6] Samios et. al., Phys. Rev. 126, 1844 (1962)
[7] Amteller et. al., Phys. Rev. **D48** 3388 (1993)
[8] Gomez Dumm, Pich, Phys. Rev. Lett. **80** 4633 (1998)